Numerical study on the pattern and origins of Kuroshio branches in the bottom water of southern East China Sea in summer

Dezhou Yang,[1,2] Baoshu Yin,[1,2] Zhiliang Liu,[1,2] Tao Bai,[3] Jifeng Qi,[1,2,4] and Haiying Chen[1,2]

Received 19 August 2011; revised 31 October 2011; accepted 30 November 2011; published 8 February 2012.

[1] Pattern and origins of Kuroshio branches in the bottom water of southern East China Sea (ECS), were carefully examined by numerical simulations based on the Regional Ocean Modeling System (ROMS) together with observations. Model results show that in the bottom water of ECS, the intrusion pattern of Kuroshio is mainly composed of an Offshore Kuroshio Branch Current (OKBC) which, bifurcated from the Kuroshio northeast of Taiwan, flows nearly along the isobath of ~100 m, and a Nearshore Kuroshio Branch Current (NKBC) which, originated from the Kuroshio northeast of Taiwan, upwells northwestward gradually from ~250 m to ~60 m, then turns to northeast around 27.5°N, 122°E, thereafter flows northeastward along the isobath of ~60 m, and finally reaches at 30.5°N where it turns to east. Furthermore, we found that the NKBC mostly originated in the Kuroshio subsurface water (120–250 m) east of Taiwan, whereas the OKBC mainly stemmed from the Kuroshio water (60–120 m) east of Taiwan. This pattern and origins of OKBC and NKBC well addressed the observational phenomena that off the coast of Zhejiang province, China, there were colder, less saline, and more phosphate-rich bottom water near the isobath of ~60 m rather than near the isobath of ~100 m in August 2009. Finally, it is proposed that on southern ECS continental shelf, Kuroshio exhibits its intrusion branches by an anticyclonical stair structure: bottom stair NKBC, middle stair OKBC, and top stair Kuroshio surface branch (KBC).

Citation: Yang, D., B. Yin, Z. Liu, T. Bai, J. Qi, and H. Chen (2012), Numerical study on the pattern and origins of Kuroshio branches in the bottom water of southern East China Sea in summer, *J. Geophys. Res.*, *117*, C02014, doi:10.1029/2011JC007528.

1. Introduction

[2] On the southern East China Sea (ECS, see Figure 1) continental shelf north of Taiwan, there is a complicated three-dimensional flow pattern in summer which could be related to the Taiwan Warm Current (TWC, see Figure 1), Kuroshio, zonal-running ECS continental shelf break northeast of Taiwan and their interaction. Generally, Kuroshio, the western boundary current of the North Pacific subtropical gyre, flows northeastward along the eastern coast of Taiwan and enters the ECS with a mean transport of 21.5 sverdrup (Sv) (1.0 Sv = 1.0 × 10^6 m^3/s) [*Johns et al.*, 2001] through the so-called East Taiwan Channel between Taiwan and Yonaguni-jima Island (YJI, see Figure 1a). As the Kuroshio flows out the East Taiwan Channel, it is blocked and deflected by the steep, zonally running ECS continental shelf break northeast of Taiwan, and then runs nearly eastward [*Liang et al.*, 2003]. In addition, near the Mien Hwa Canyon (MHC, see Figure 1a) there are two northwestward Kuroshio intrusion branches: north branch and south branch [*Hsueh et al.*, 1992; *Qiu and Imasato*, 1990; *Tang et al.*, 2000]. The north branch is called Kuroshio branch current (KBC, see Figure 1b), which intrudes into the ECS continental shelf through the North Mien Hwa Canyon (NMHC, see Figure 1) [*Qiu and Imasato*, 1990; *Tang et al.*, 1999; *Wong et al.*, 2000]. However, the KBC in the upper layer in summer, mostly turns to ESE near 27°N and rejoins the mainstream of the Kuroshio [*Hu et al.*, 2008; *Qiu and Imasato*, 1990], which is due, in part, to the Ekman drift associated with the southwest monsoon that impedes the landward movement of the Kuroshio surface water and, in part, to the preponderance of the less dense water from the Taiwan Strait (TS) and coastal regions of China, which also impedes the intrusion of the Kuroshio surface water [*Hsueh et al.*, 1992, 1993]. On the other hand, the south branch makes a cyclonic turning (see the circled number one in Figure 1a), and rejoins the Kuroshio off the northeastern tip of Taiwan [*Chuang et al.*, 1993; *Hsueh et al.*, 1992, 1993; *Liu et al.*, 2000; *Tang and Yang*, 1993; *Tang et al.*, 1999], and gives rise to a cold eddy around the MHC with a diameter of about 70 km [*Chuang et al.*, 1993; *Tang et al.*, 1999] where the upwelling

[1]Key Laboratory of Ocean Circulation and Waves, Chinese Academy of Sciences, Qingdao, China.
[2]Institute of Oceanology, Chinese Academy of Sciences, Qingdao, China.
[3]North China Sea Marine Forecasting Center, State Oceanic Administration, Qingdao, China.
[4]Graduate School, Chinese Academy of Sciences, Beijing, China.

0148-0227/12/2011JC007528

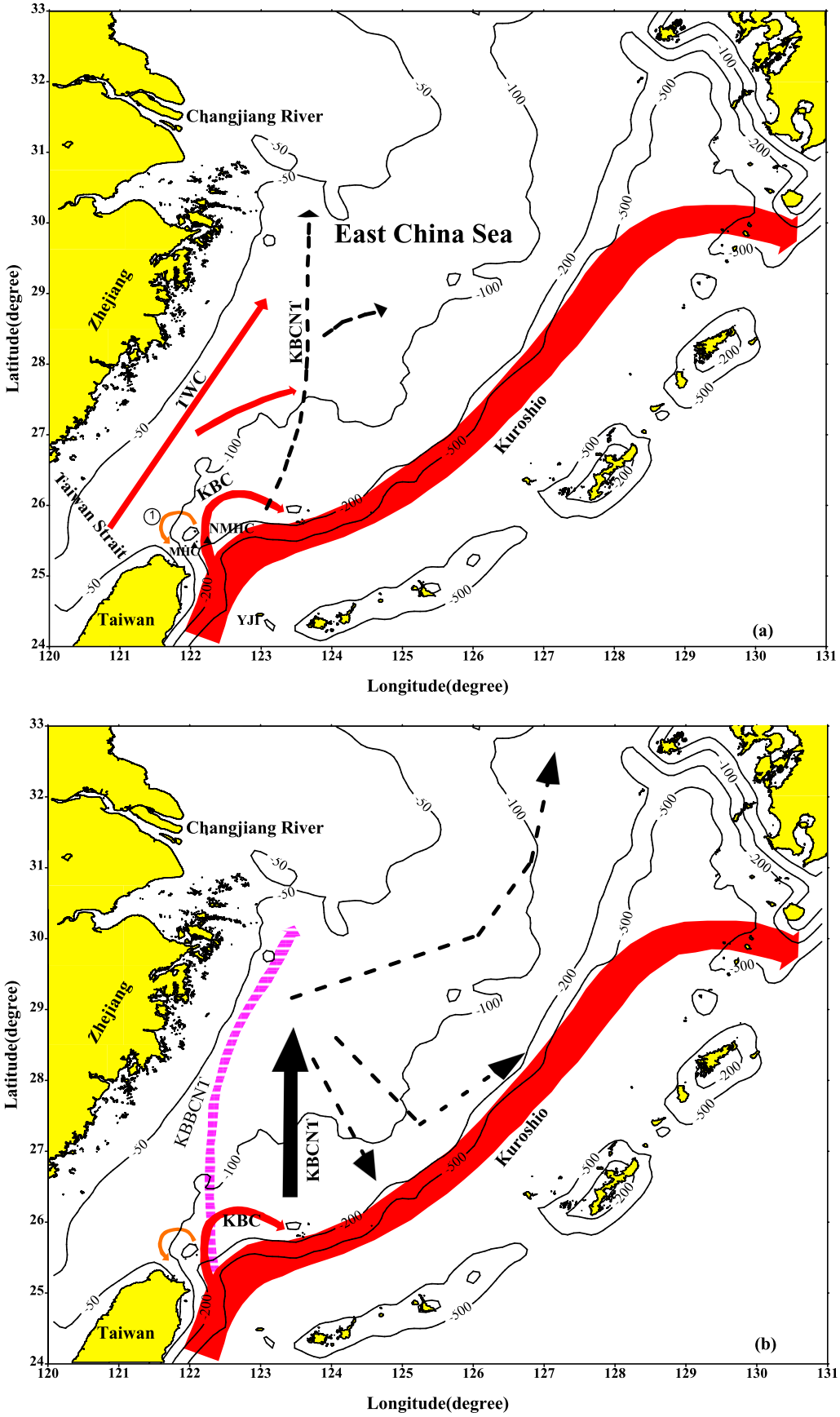
Changjiang River
East China Sea
Zhejiang
Taiwan Strait
TWC
KBCNT
KBC
NMHC
MHC
Kuroshio
Taiwan
YJP
(a)
KBBCNT
KBCNT
KBC
Kuroshio
Taiwan
(b)
Latitude(degree)
Longitude(degree)

Figure 1

of the Kuroshio subsurface water is a permanent feature that occurs the whole year [*Chen et al.*, 1995; *Liang et al.*, 2003; *Liu et al.*, 1992; *Wong et al.*, 2000]. But the countercurrent in summer is sometimes not visible, which can be attributed to the variation of Kuroshio [*Chang and Oey*, 2011; *Zhang et al.*, 2001]. The Kuroshio branch pattern near Taiwan has been well examined by some projects such as Kuroshio edge exchange processes (KEEP), a part of the Joint Global Ocean Flux Study [*Wong et al.*, 2000], but the KBC pattern further north of Taiwan remains unclear because of absence of observations (for example, KEEP is limited to area south of 26.5°N).

[3] As for the Kuroshio branches further north of Taiwan, *Kondo* [1985] proposed that on the southern ECS continental shelf, there was a nearly northward current, which was separated from the Kuroshio northeast of Taiwan, flowed roughly along the meridian of 123.5°E, and could reach 30.0°N. This current is called KBC north of Taiwan (KBCNT, see Figure 1a) or "Kuroshio Separation," which exists throughout the year. In addition, a small eastward or northeastward bifurcation may occur from the KBCNT near 28°N. The KBCNT presented by *Kondo* [1985] was based on an analysis of mean distribution of water properties at 50 m, and its position is further offshore than that of the TWC [*Guan and Fang*, 2006]. According to *Ichikawa and Beardsley* [2002] (see their Figure 10), the KBCNT north of 29°N does not exist, which is replaced by a northeastward flow roughly along the isobath of ~100 m (see dash line arrows in Figure 1). Furthermore, to the east of the KBCNT (see Figure 1b) there are two currents that flow southeastward and transport the ECS continental shelf water to the left side of Kuroshio. In contrast, it was pointed out that there were no Kuroshio branches but the dominative TWC on the southern ECS continental shelf, and the deep water of TWC originated in Kuroshio subsurface water [*Guan and Fang*, 2006; *Su et al.*, 1994]. The Kuroshio intrusion pattern in the deep water of ECS was not elucidated in their results because of the absence of direct current observations. Recently, *Yang et al.* [2011] proposed that in the deep and bottom water of ECS, there is a Kuroshio bottom branch current north of Taiwan (see KBBCNT in Figure 1b), which links the Kuroshio subsurface water near MHC to the bottom water off Changjiang river mouth. Nevertheless, the detailed pattern of Kuroshio intrusion currents around the southern ECS continental shelf edge between isobath of 100 m and isobath of 200 m is still unknown [*Isobe*, 2008].

[4] However, there are some studies, which imply the possible intrusion of Kuroshio onto the southern ECS continental shelf. It was reported by *Tang et al.* [1999] and *Wong et al.* [2000] that the KBC immediately north of MHC in vertical direction turns gradually with depth to west; in other words, the KBC flows northeastward at top layer but at the bottom layer it flows westward. This current structure in vertical direction implies that the current at the middle layer maybe flows northwestward and impinges onto the ECS continental shelf. In addition, it was further pointed out that the cross-shelf intrusion of the Kuroshio in summer would seem most likely near the seafloor [*Hsueh et al.*, 1993]. In addition, a cold water mass is often found to the west of the KBC (see Figure 1), which has hydrographic properties similar to the Kuroshio subsurface water at ~300 m [*Tang et al.*, 1999]. Therefore, it seems reasonable that there are Kuroshio intrusion branches that originate from the Kuroshio subsurface water near MHC, then flow generally northwestward, and impinge onto the southern ECS continental shelf carrying the saline and cold Kuroshio water through the canyon immediately north of MHC.

[5] Despite recent progress, the Kuroshio branches in the deep water of ECS north of 26°N and their origins remain to be elucidated. Different opinions of Kuroshio intrusion branches and their origins mainly come from the absence of observational data and a numerical model, which is robust enough to capture the main features of the Kuroshio intrusion branches [*Ichikawa and Beardsley*, 2002]. In this article, the KBBCNT (Figure 1b) is further checked by observational temperature and phosphate distributions, and the dynamic of the generation and sustaining mechanism of KBBCNT (Figure 1b) is analyzed in detail. In addition, a high-resolution model in combination with observations from a summer cruise covering the whole southern ECS has been employed to investigate the possible Kuroshio intrusion branches and their origins.

2. Observational Phenomena About Kuroshio Intrusion in Summer

[6] Thirty-two stations were occupied by an ECS summer cruise conducted by the Xiamen University in the period between 15 August and 2 September 2009 along four transects normal to the coast of the ECS (Figure 2). The profiles of temperature and salinity were measured by conductivity-temperature-depth sensors. Nutrient samples collected from observation stations at different depths were filtered using 0.45 μm acetate fiber membrane, and then analyzed using a Technicon AA3 autoanalyzer (BRAN-LUEBBE) onboard, according to classical colorimetric methods [*Grasshoff et al.*, 1983]. The samples were analyzed immediately, or refrigerated at 4°C and then analyzed within 50 hours upon sampling.

[7] Figure 3a shows two cold cores (core1 and core2, see Figure 3a) in the bottom water of transect DH3 in August 2009. To our surprise, the temperature of core1 is 1° lower than that of core2, but the depth of core2 is ~30 m deeper than that of core1. This phenomenon seems to be opposite to our common sense that the deeper the water depth is, the colder the water is. With respect to salinity in the bottom water, the maximum, with a value higher than 34.6, is found in core2, but it decreases slowly to 34.35 at station DH35, and then steadily increases to 34.43 in core1. In summer, the water of TS, with high temperature and low salinity, rushes out of the TS, forming the TWC (see Figure 1), and

Figure 1. Summer Kuroshio branch pattern in the ECS where isobaths of 50 m, 100 m, 200 m, and 500 m are overlapped. The circled number one indicates counterclockwise circulation around MHC [*Chuang et al.*, 1993; *Hsueh et al.*, 1992]. KBCNT in Figure 1a was given by *Kondo* [1985]; KBCNT and dash line arrows in Figure 1b came from *Ichikawa and Beardsley* [2002]; KBC indicates the Kuroshio Branch Current [*Qiu and Imasato*, 1990]; KBBCNT was proposed by *Yang et al.* [2011].

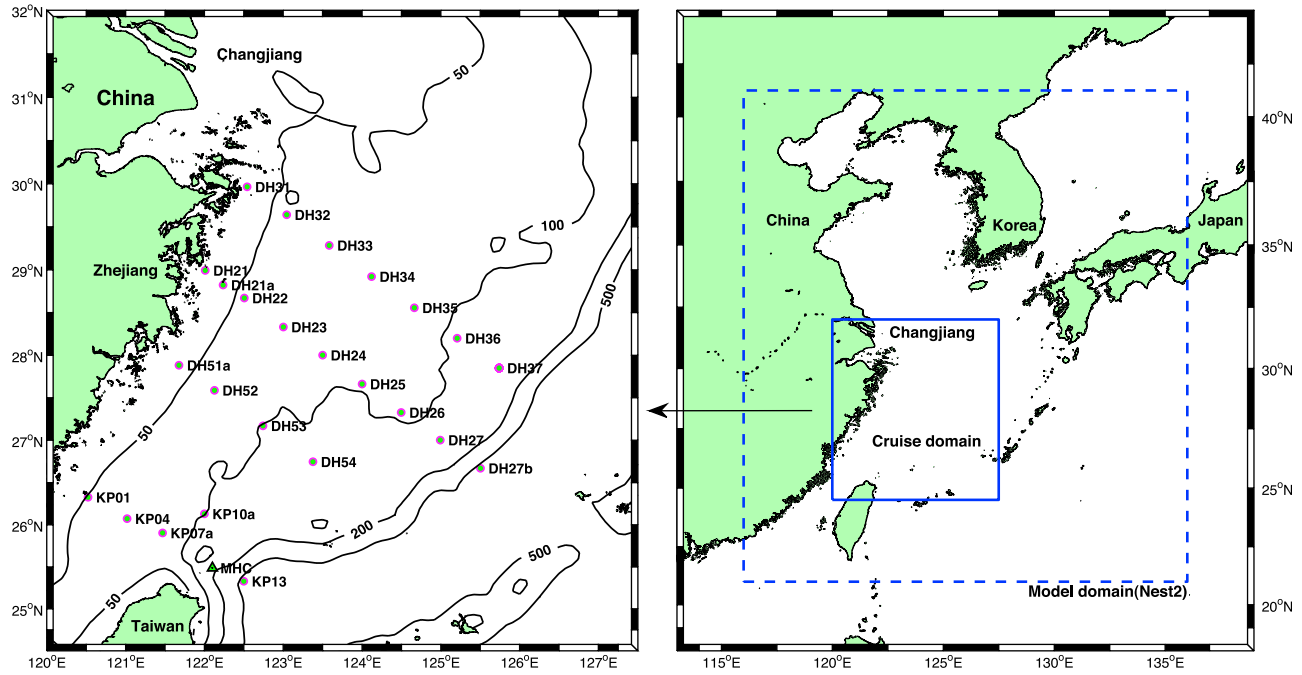

Figure 2. (left) Sampling stations in August 2009 and (right) model domain (Nest2, enclosed area by dashed line). Figure 2 (left) is the enlarged cruise domain depicted by the solid line box in Figure 2 (right). Transect KP comprises KP01, KP04, KP07a, KP10a, and KP13; transect DH5 comprises DH51-DH53; transect DH3 comprises DH31-37, and transect DH2 comprises DH21-27. In Figure 2 (left), the thin solid lines represent the contour lines (500 m, 200 m, 100 m, and 50 m) of topography.

flows northeastward only in the surface water above the depth of ~60 m on the southern ECS continental shelf [*Guan and Fang*, 2006; *Hu et al.*, 2010] as the depth in the northern-end part of the TS is less than 60 m (see Figure 2). Next, the northeastward-flowing TWC goes through the central part of transect DH3. In addition, the TWC water (TWCW, see Figures 3a and 3b), which has a characteristic value of salinity of 33.7~34.2 and temperature of 23°C–29°C [*Su and Wong*, 1994], below the depth of 60 m all but disappears because of the buoyancy blocking caused by the bottom dense water. Therefore, it is immediately clear that the saline water in core1 and core2 does not derive from the water of TS. It has been reported that the bottom saline water in transect DH3 comes mainly from the Kuroshio subsurface water east of Taiwan [*Su et al.*, 1994; *Su and Wong*, 1994]. Even so, one question still arises: why does the temperature and salinity of core1 appear to be lower than that of core2?

[8] The characteristic temperature and salinity of the Kuroshio water east of Taiwan are displayed by the temperature and salinity profiles (see Figures 3d and 3e) at station KP13, the location of which is shown in Figure 2. In Figure 3e, when compared to Figure 3b, it is worth noting that the salinity (~34.5) of core1 in transect DH3 is comparable to the salinity at the depths ~60 and ~250 m at station KP13, respectively, while the salinity (~34.6) of core2 is comparable to the salinity at ~90 m at station KP13. With respect to core1, it is obvious that the salinity of core1 cannot derive from the Kuroshio water near the depth of ~60 m, as no forcing can drive the Kuroshio water above 60 m to break the blocking of TWC, which flows northeastward and is dominant in the upper 60 m on the southern ECS continental shelf in summer. It follows then that the most probable origin of core1 is the Kuroshio water near the depth of ~250 m. In contrast, core2 stems mainly from the Kuroshio water near the depth of ~90 m. This opinion is immediately confirmed by the observational fact that core1 is colder than core2, although the water temperature between ~120 and ~250 m at station KP13 (see Figure 3d) is ~3°C–5°C colder than that in core1 and core2. However, the ~3°C–5°C difference of temperature is reasonable because of the strong tidal mixing and other physical factors. Nevertheless, the salinity cannot equally achieve the same mixing as temperature because of the more rapid diffusion of temperature relative to the salinity [*Large et al.*, 1994]. In light of the above comparisons of temperature and salinity between transect DH3 and station KP13, it should come as no surprise that Kuroshio water at ~250 m east of Taiwan flows into the transect DH3, forming the saline and cold core1, while the core2 originates in the Kuroshio water at ~90 m east of Taiwan, which is salty and warm relative to the water at ~250 m (see Figures 3d and 3e). This opinion is also confirmed by the distribution of $[PO4]^{3-}$ in Figures 3c and 3f. The concentration value of $[PO4]^{3-}$ at ~250 m at station KP13 (see Figure 3f) corresponds strikingly to the value in core1 (see Figure 3c), and the concentration value of $[PO4]^{3-}$ in core2 is highly consistent with that of Kuroshio water at ~90 m. In addition, it is interesting to note is that the cold water area enclosed by the temperature contour of 19°C in Figure 3a is almost identical to the area enclosed by the salinity contour of 34.43 in Figure 3b as well as the area enclosed by $[PO4]^{3-}$ contour of 0.86 mmol/m^3 in Figure 3c. Although there are chemical and biological reasons to cause

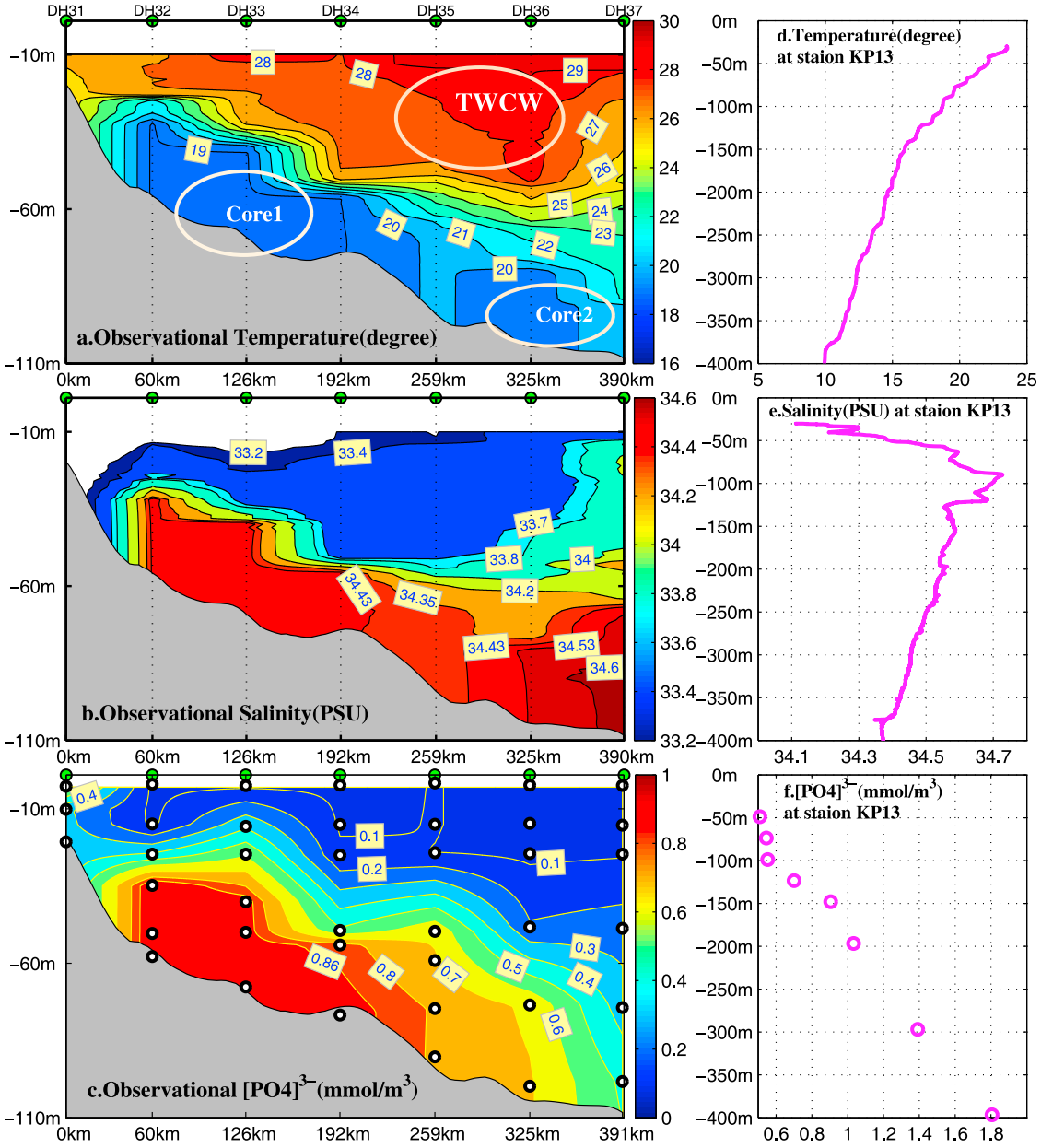

Figure 3. Distributions of (a) temperature, (b) salinity, and (c) phosphate ($[PO4]^{3-}$) along transect DH3, and profiles of (d) temperature, (e) salinity, and (f) phosphate ($[PO4]^{3-}$) at sampling station KP13 (see Figure 2). TWCW denotes Taiwan Warm Current Water.

variation of the phosphate concentration in core1 and core2, until oceanic biological and chemical processes are observed and quantified, the assumption that the phosphate of core1 and core2 derive from the ~250 and ~90 m Kuroshio subsurface water east of Taiwan, respectively, will remain appropriate.

[9] However, above and beyond all these, a problem arises: how does the Kuroshio subsurface water east of Taiwan reach the transect DH3? It was reported that the Kuroshio subsurface water appeared only along 123°E in an area north of 28°N [*Su and Wong*, 1994] in summer. In their opinion, the bottom saline and cold water in transect DH3 came mainly from the Kuroshio north of 28°N, which upwelled near the ECS continental shelf break and intruded westward. In contrast, *Hu et al.* [1984] pointed out that, in summer, core1 was caused by the upwelling of deep water, and that the upwelling was not wind driven but controlled by a possible branch of Kuroshio. *Yang et al.* [2011] elucidated further that it was caused by a bottom Kuroshio branch that bifurcated from the Kuroshio subsurface water northeast of Taiwan, and reached 30.5°N off Changjiang river mouth, forming the bottom saline water off the coast of Zhejiang province, China (see Figure 2). However, whether or not there is another Kuroshio branch that might have caused the core2, remains an unanswered research question.

[10] Figures 4a and 4b show the horizontal distributions of observational salinity at bottom layer and at 90 m depth,

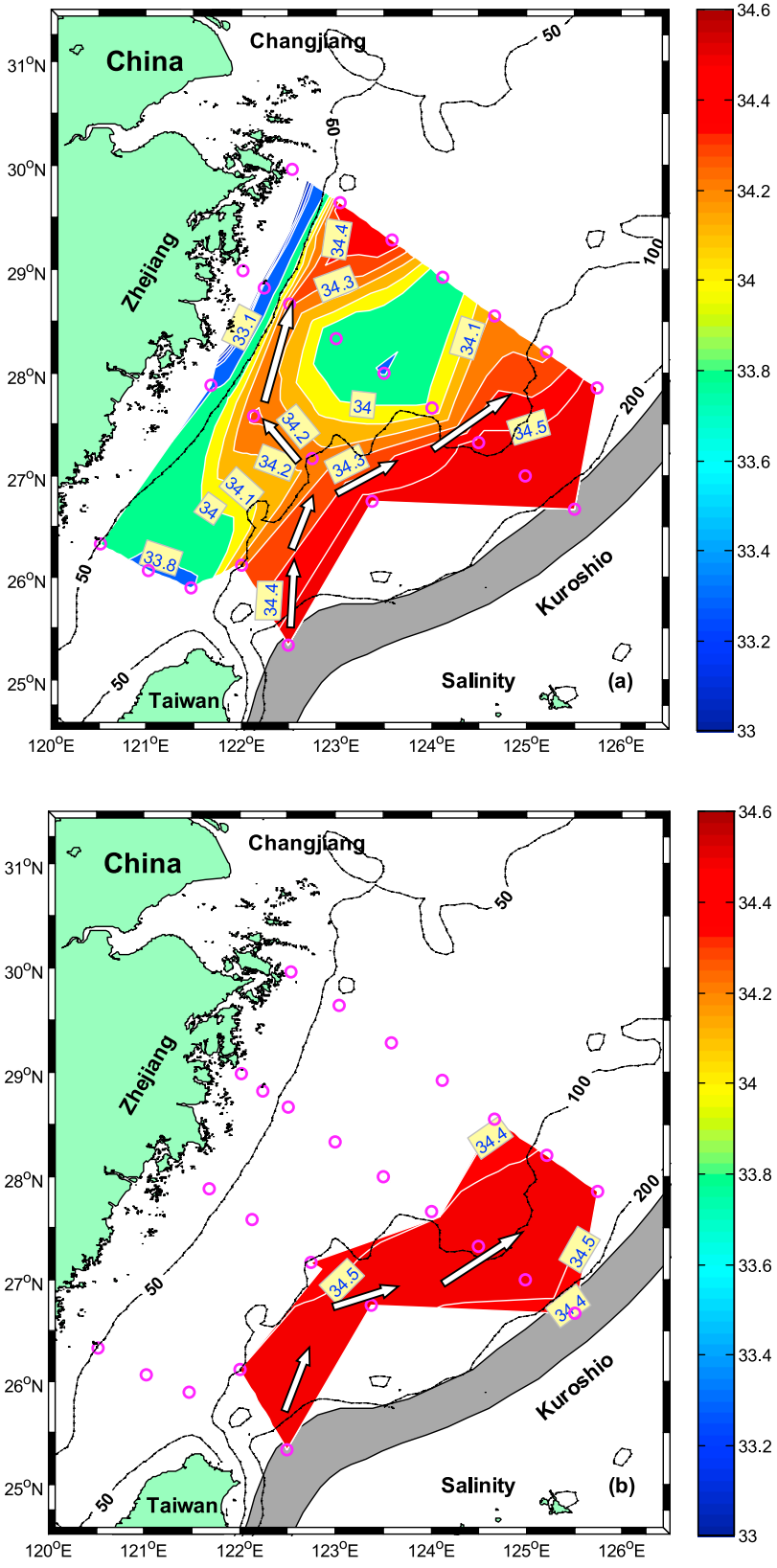

Figure 4. Distributions of observational salinity (a) near bottom layer and (b) at 90 m depth where the isobaths of 50 m, 100 m, and 200 m are overlapped. Gray area denotes typical Kuroshio path, and arrows imply the Kuroshio branches.

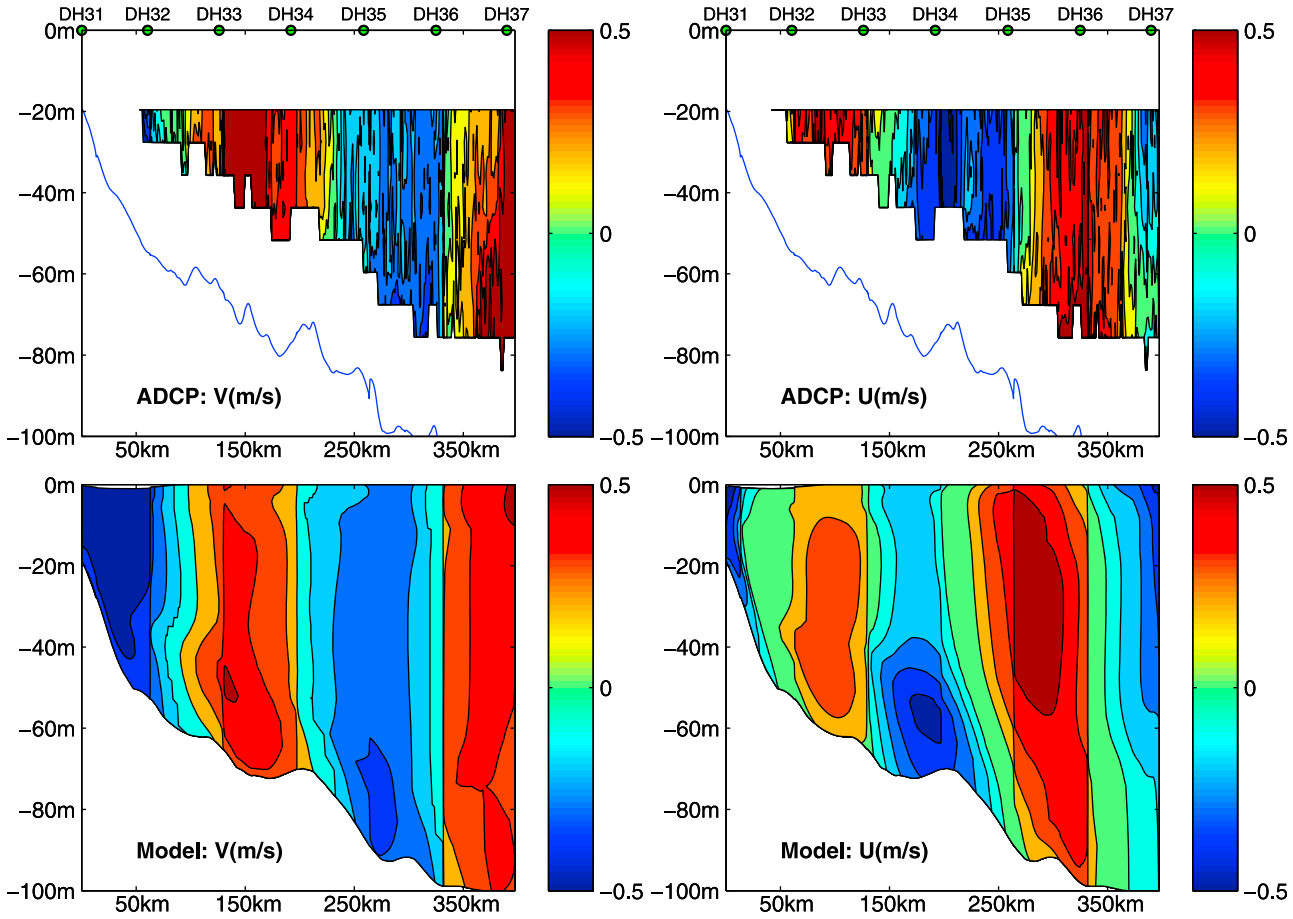

Figure 5. Current velocity (U eastward is positive and V northward is positive) comparison between model results and observations from a Ship-board Acoustic Doppler Current Profiler (SADCP) which moved continuously from station DH37 to station DH31 between 21 and 22 August 2009. The thin solid lines in Figure 5 (top) represent the bottom depth measured by SADCP.

respectively. It can be easily found that, at the bottom layer, the saline waters in core1 and core2 of transect DH3 are both linked continuously to the mainstream of Kuroshio immediately to the northeast of Taiwan. In addition, in Figure 4b the Kuroshio subsurface water east of Taiwan seemingly are transported downward to core2 by a Kuroshio branch that appears to closely follow the 100 m isobath. Therefore, it may be assumed that the core2 in transect DH3 is caused by an offshore KBC (OKBC), and core1 in transect DH3 is formed by a nearshore KBC (NKBC, which is identical to KBBCNT in Figure 1, but hereafter, KBBCNT is called NKBC for consistence with KBC and OKBC). NKBC orientates in the Kuroshio water at ~250 m east of Taiwan [*Yang et al.*, 2011], and can passes through (see the KBBCNT [*Yang et al.*, 2011] in Figure 1b) core1 of the transect DH3 where it causes the colder, less saline, and more phosphate-rich water than that in core2. At the same time, the OKBC, bifurcated from the Kuroshio water near ~90 m northeast of Taiwan, flows along the isobath of ~100 m, mostly passes through core2 of transect DH3 (part of OKBC maybe rejoin the Kuroshio mainstream at 28°N), and as a result, causes the warmer, more saline, and less phosphate-rich water in core2 relative to the water in core1. For these reasons, it is most reasonable that in the deep water of southern ECS, the Kuroshio intrusion pattern is mainly composed of NKBC and OKBC, as they can well address the question: why is there a colder, less saline, and more phosphate-rich water in core1 of transect DH3 when compared to core2 of transect DH3. Also, from Figures 4a and 4b, it is evident that the pathways of NKBC and OKBC can be traced by the high salinity water (see the arrows in Figures 4a and 4b). However, the absence of direct current measurements is obvious in this area.

[11] Figure 5 shows the measured current by the Ship-board Acoustic Doppler Current Profiler (SADCP, whose system frequency is 76.8 kHz, bin size is 8 m, and first bin range is −16.57 m), which moved continuously from the station DH37 to station DH31 between 21 and 22 August 2009. However, the SADCP data gives no further information about the bottom intrusion current but the dominant tide current. In addition, it is almost impossible to filter the high-frequency tidal current from this SADCP data. Fortunately, either the magnitude or the pattern of the observational current is comparably reproduced by our model results (see Figure 5, bottom). Next, the high-resolution numerical model, which is based on Regional Ocean Modeling System (ROMS), is employed to examine the pattern of the Kuroshio branches: NKBC and OKBC.

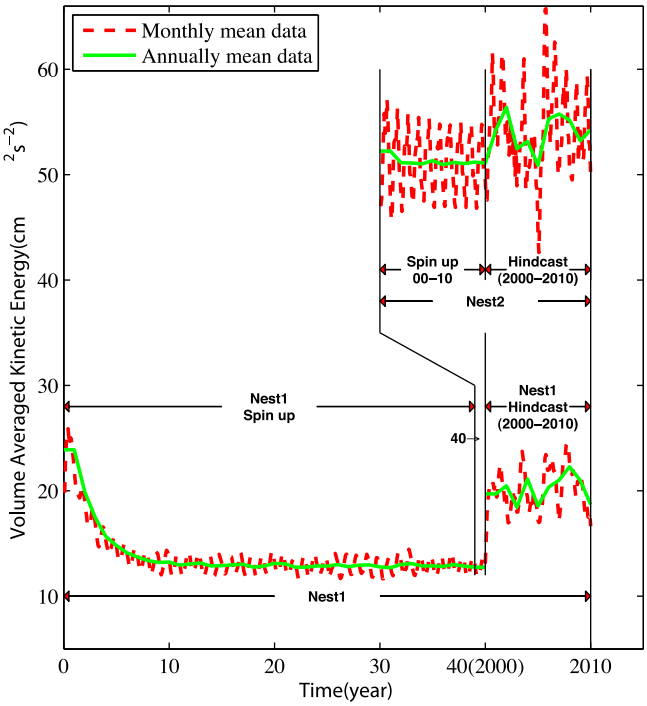

Figure 6. Time evolution of the volume-averaged kinetic energy in Nest1 and Nest2 together with the procedure employed to deal with the one-way nesting simulation.

3. Numerical Simulation of the Kuroshio Intrusion Branches

[12] The ROMS belongs to a general class of three-dimensional, free surface, terrain-following [*Song and Haidvogel*, 1994] numerical models applicable to oceanographic and estuarine studies. The hydrostatic primitive equations resulting from Reynolds averaging of the Navier–Stokes equations are solved in ROMS. Although ROMS offers many methods to implement turbulence closure, in this article, the horizontal and vertical eddy viscosity are calculated using the Smagorinsky parameterization and the K-profile parameterization (KPP) schemes [*Large et al.*, 1994], respectively. Details of the ROMS computational algorithms are reported by *Shchepetkin and McWilliams* [2005].

3.1. Model Configuration

[13] Regional oceanic models can be developed and used efficiently for the investigation of regional and coastal domains, provided a satisfactory prescription for the open boundary conditions is found [*Marchesiello et al.*, 2001], which, however, is the classic dilemma in regional ocean modeling. Therefore, to obtain appropriate open boundary conditions for the region of Kuroshio on the ECS continental shelf, we first run a ROMS Pacific model (98°E–112°W, 40°S–67°N, see nest1 of Figure 2 in *Yang et al.* [2011]), and then a one-way nesting procedure (see Figure 6) is employed whereby 5 day average temperature, salinity, and baroclinic velocity from the nest1 simulation are imposed at the oceanic perimeter of a high-resolution nest2 model (116°E–136°E, 21°N–41°N, see nest2 in Figure 2, right). The depth–average velocity and sea surface height (SSH) boundary conditions are used to allow the outward radiation of gravity waves generated within the nest2 domain without upsetting the perimeter temperature and salinity fluxes [*Marchesiello et al.*, 2001]. In nest1 model, 26 *s*-coordinate levels are used in the vertical direction, and the horizontal resolution is ~18 km (1/6° × 1/6°cos Φ, where Φ is latitude), as a horizontal grid size of 20 km at ~30°N is a threshold to the proper representation of Kuroshio extension and separation [*Hasumi et al.*, 2010]. The nest2 model has been implemented with the same vertical resolution as the nest1 but with a higher horizontal resolution of ~8 km (1/12° × 1/12° cos Φ, where Φ is latitude). A stretching method of the vertical grid introduced by *Shchepetkin and McWilliams* [2009] has been used to increase resolution near the surface and bottom boundaries.

[14] Figure 6 demonstrates the time evolution of volume-integrated kinetic energy (KE) of nest1 and nest2 models and illustrates the strategy employed to deal with the one-way nesting simulation. According to the decreasingly oscillating KE around the equilibrium value, the spin-up times are long enough to the hindcast run of nest1 and nest2 models. For spin-up of nest1 model, it has been integrated for 40 years, and then a hindcast run (2000–2010) of nest1 is carried out to provide open boundary conditions for nest2. Next, for spin-up of nest2 model, it is initialized with a state of nest1 model at 1 January, 40th model year (see Figure 6), and then has been run for 10 model years forced at boundaries with spin-up results of nest1 in the 40th model year. The hindcast (2000–2010) run of nest2 is forced at the boundaries with interpolated 5 day mean fields from hindcast (2000–2010) run of nest1 model, and with tidal velocities and free-surface heights from 10 tide constituents of the TPXO7 [*Egbert and Erofeeva*, 2002]. In addition, coastal freshwater input is applied using observed river flow data from Changjiang River. It is worth noting that in this article, the salinity of Changjiang River is set to 2 rather than the interpolated value from coarse monthly mean climatology salinity [*Yang et al.*, 2011] because the horizontal resolution of climatology salinity is so coarse (1° × 1°) that the interpolated salinity (>30) of Changjiang River is unreasonable.

[15] For further particulars of topography, nudging configuration, and forcing data, such as heat flux, water flux, momentum flux, and salinity flux, used by spin-up run and hindcast run of nest1 and nest2 models, please refer to our earlier article [*Yang et al.*, 2011]. In this article, we only focus on the analysis of the model results.

3.2. Model Results

[16] Figure 7 illustrates the monthly mean current at 20 m depth from nest1 hindcast run in August 2009, corresponding to our summer cruise conducted in August 2009. It is interesting to note that the Kuroshio properly separates from the eastern coast of Japan around 35°N [*Hasumi et al.*, 2010] rather than unfortunately overshoots to north along the east coast of Japan to 40°N [*Guo et al.*, 2003], and then continues to flow eastward as the Kuroshio extension current. Also evident is that the southward intrusion of the Oyashio along the east coast of Japan is reproduced appropriately (see Figure 7). As reported by *Hasumi et al.* [2010], the success of north Pacific modeling hinges on the proper representation of the Kuroshio separation. Therefore, the nest1 model is strong enough to supply appropriate boundary and initial conditions to the nest2 model. In addition, our purpose is to investigate the Kuroshio branches and their origins

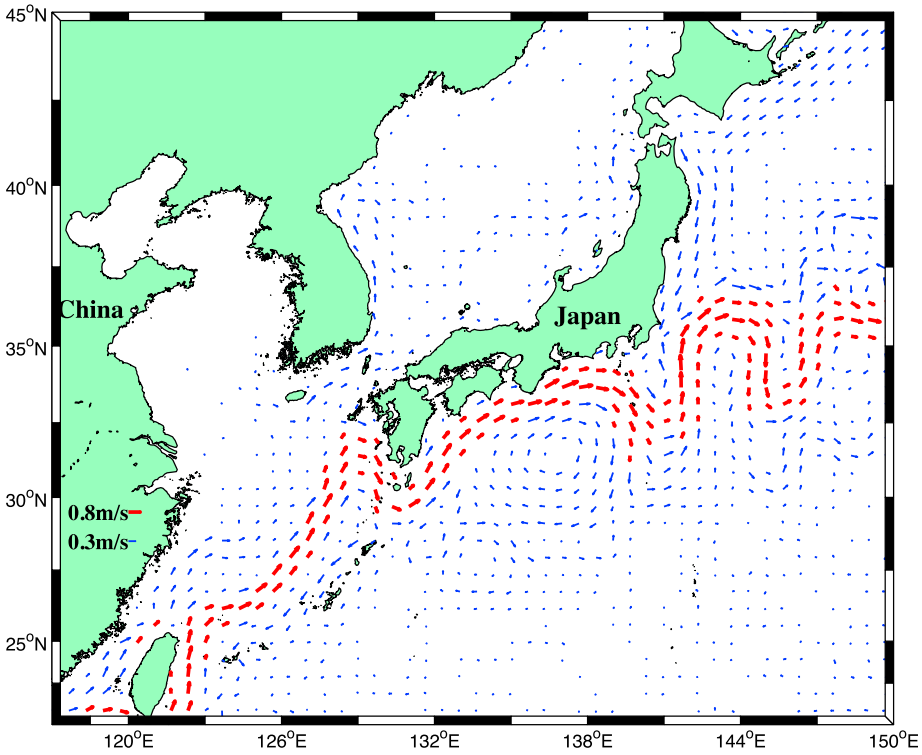

Figure 7. Monthly mean current at 20 m depth from Nest1 hindcast run in August 2009.

in summer; therefore, the simulation is evaluated with a particular focus on Kuroshio on the ECS continental shelf in summer.

[17] Figure 8 shows the monthly mean current at 20 m depth from nest2 hindcast run in August 2009. The modeled ocean circulation pattern in Figure 8, agrees well with the known circulation structure on the ECS continental shelf

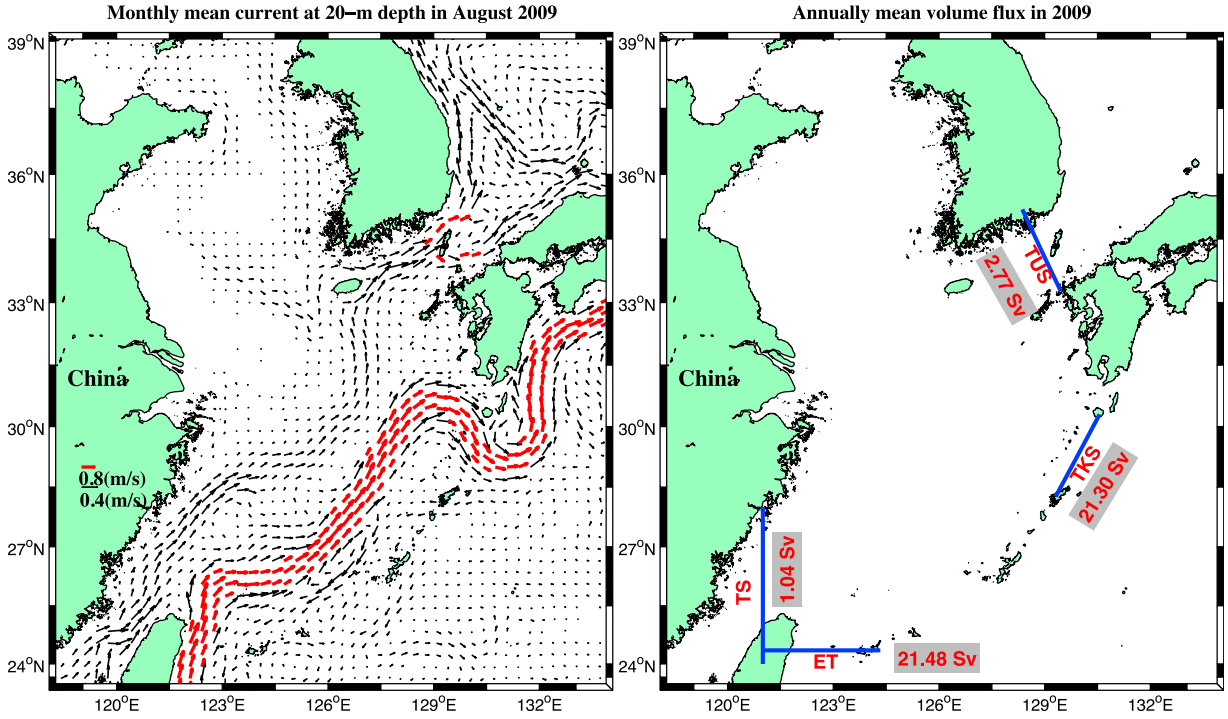

Figure 8. (left) Modeled monthly mean current at 20 m depth from Nest2 hindcast run in August 2009, and (right) modeled annually mean volume flux across Taiwan Strait (TS), East of Taiwan (ET), Tsushima Strait (TUS), and Tokara Strait (TKS) from Nest2 hindcast run in 2009.

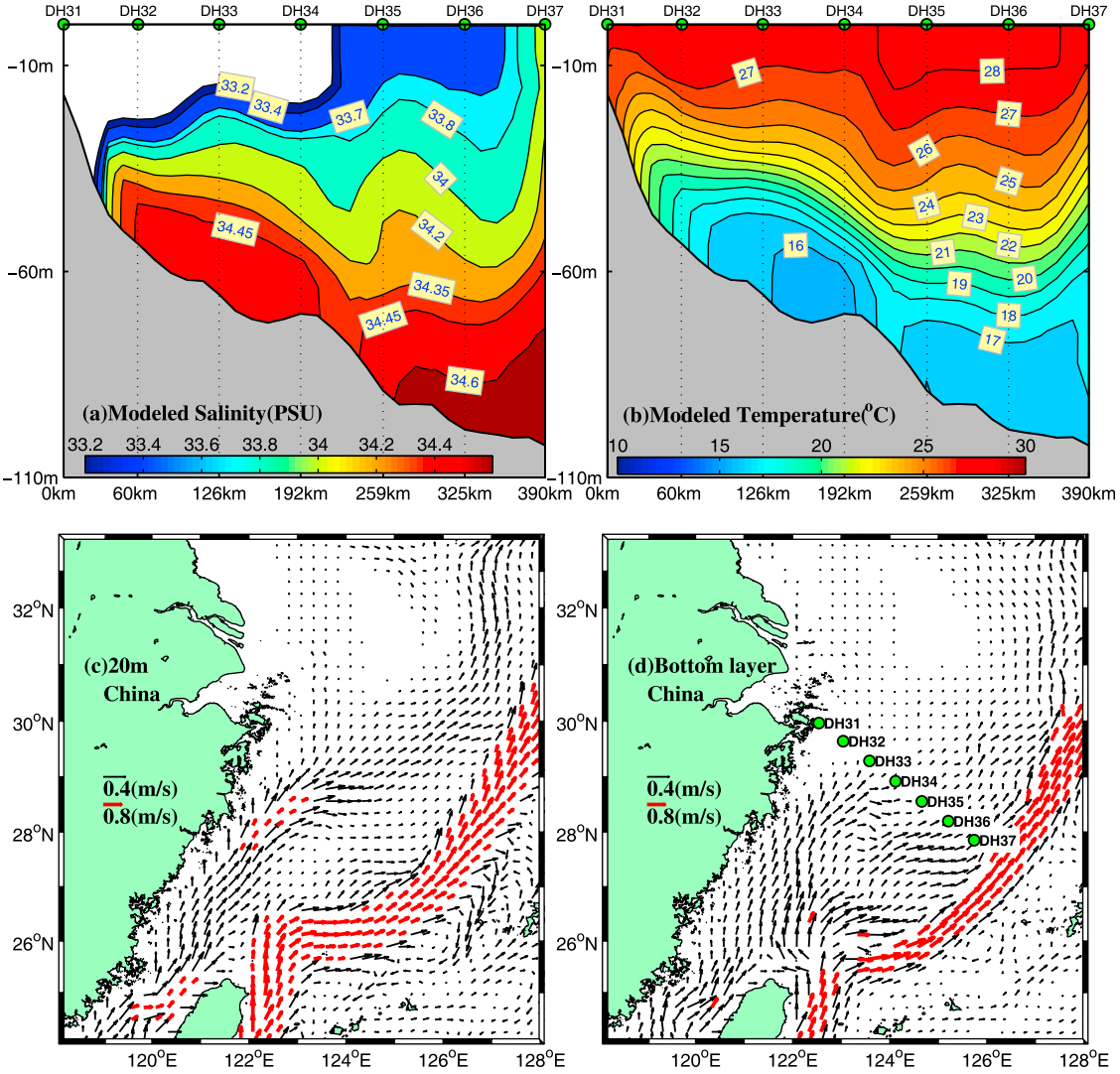

Figure 9. Modeled 5-day (20–25 August 2009) average (a) salinity and (b) temperature distributions along transect DH3 from Nest2 hindcast run; and modeled monthly mean current (August 2009) at (c) 20 m depth and (d) bottom layer along with the station locations of DH3. In Figure 9d, the bottom current where depth is deeper than 200 m, is replaced by the current at 200 m depth.

such as Kuroshio and TWC [*Guan and Fang*, 2006] in summer. As for the Kuroshio pattern on ECS continental shelf, there is a remarkable agreement between observations [*Hu et al.*, 2008; *Ichikawa and Beardsley*, 2002; *Qiu and Imasato*, 1990] and modeled results where the Kuroshio turns northeastward northeast of Taiwan and flows along the shelf break until ~30.5°N where it turns eastward and then exits the ECS through the Tokara Strait (TKS). The strength and width of the modeled Kuroshio by nest2 model are about 1 m s^{-1} and 100 km, respectively. Also, in summer, it is evident that the TWC mainly originates from TS and flows northeastward on the ECS continental shelf [*Guan and Fang*, 2006]. Although there is a little overshooting of Kuroshio west of TKS in nest1 model, the Kuroshio modeled by nest2 turns properly to east at ~30.5°N. Horizontal resolution is believed to be essential to the generation of a little overshooting of Kuroshio west of TKS [*Guo et al.*, 2006].

[18] Furthermore, a quantified verification of nest2 model is also provided in this article by comparisons between observed and modeled volume fluxes (see Figure 8) across TS, Tsushima Strait (TUS), TKS, and a section East of Taiwan (ET). On the basis of hindcast run in 2009, nest2 model provides the annually mean volume flux 1.04 Sv for TS, 2.77 Sv for TUS, 21.48 Sv for ET, and 21.30 Sv for TKS (see Figure 8), which agree quantitatively with observations 1.20 Sv across TS [*Isobe*, 2008], 2.65 Sv across TUS [*Takikawa et al.*, 2005], 21.45 Sv across ET [*Johns et al.*, 2001], and 20.00 Sv across TKS [*Teague et al.*, 2003], respectively.

[19] Modeled 5 day average salinity and temperature distributions along transect DH3 from nest2 hindcast run (20–25 August 2009) are shown in Figures 9a and 9b, respectively. It is clearly shown that the core1 and core2 in transect DH3 are occupied by saline water, and the salinity value of core1 is less than that of core2, which are consistent

with the observations in Figure 3b. Furthermore, the poor agreement between modeled salinity and observations in the upper layer of transect DH3 (see Figure 11 in *Yang et al.* [2011]) has been significantly improved. The agreement between modeled temperature pattern (Figure 9b) and observational temperature pattern (Figure 3a) is remarkably good, although modeled temperature of core1 and core2 is ∼2°C less than the observations, which may be caused by the insufficient mixing of KPP scheme at particular depth [*Large et al.*, 1994]. To our surprise, not only each core in Figure 3a is faithfully represented (see Figure 8b), but also the colder core1 when compared to core2 is also well reproduced by the nest2 model. For these reasons, it is reasonable that the nest2 model is accurate enough to produce realistic current field on the ECS continental shelf. The nest2 model is further confirmed by the good agreement between the modeled current and the observational current data from SADCP (see Figure 5).

[20] Figures 9c and 9d illustrate modeled monthly mean current at 20 m depth and bottom layer from nest2 hindcast run in August 2009, respectively. In Figure 9c, the monthly mean current at 20 m depth, shows a prominent feature of TWC, which originates in the TS and flow northeastward, transporting the warm and low-salinity TS water into the central part of transect DH3 (see Figures 3a and 3b). However, in Figure 9d the strong northwestward intrusion dominates on the ECS continental shelf, but the TWC only can be seen in a narrow area close to the coast of China and almost disappears to the north of 28°N. Interestingly, two currents are clearly shown in Figure 9d: one current flows northwestward and can reach station DH33, while the other one flows first northwestward, then turns to northeast, and finally reaches station DH36. In addition, it is worth bearing in mind that the station DH33 and DH36 are exactly the locations where core1 and core2 are found, respectively. According to *Chuang et al.* [1993], *Hsueh et al.* [1992, 1993], *Liu et al.* [2000], *Tang and Yang* [1993], and *Tang et al.* [1999], there is a westward current immediately northeast of Taiwan, which is also reproduced in Figure 9d. Thus, these features of bottom intrusion currents in Figure 9d clearly support our assumption that core1 and core2 in Figure 3a are caused by different currents. Next, further numerical experiments have been conducted to discuss the intrusion currents and their origins.

4. Discussion

[21] A particularly encouraging result of the nest2 model is that the nest2 model is capable of reproducing the observational fact that there are two saline and cold cores in the bottom water of transect DH3, and especially the observational phenomenon that the water of core1 has colder temperature and lower salinity than that of core2. This success depends on the capability of the nest1 model to provide the nest2 model with accurate open boundary conditions, and on the recent improvement in both the resolution and the accuracy of forcing data based on satellite product. On the basis of the nest2 model, particles tracking and passive tracer experiments are conducted to examine closely the OKBC and NKBC. Of particular interest here are their origins and their paths. In addition, not only the generation mechanism of the NKBC and OKBC but also the sustaining mechanism of the NKBC, is discussed in the following sections.

4.1. Particles Tracking and Passive Tracer Experiments

[22] Particles tracking and passive tracer experiments have been carried out to confirm our assumption that the NKBC originates in a deeper water when compared to OKBC, and results in the colder and less saline water in core1 relative to core2. Particles tracking experiment began on 1 July 2009, which is almost one month earlier than the cruise time of Transect DH3 because it will take nearly one month for the water east of Taiwan to reach Transect DH3. Along the Tracer and Particles Releasing Section (TPRS, see Figure 10), the particles 1, 2, 3, and 4 are released at the depth of ∼80, ∼250, ∼260, and 220 m, respectively. At the same time, the tracer experiment started on 1 July 2009, and from 1 July to 1 October 2009, the tracer value in a particular area along TPRS (see the filled red area in Figure 10) is fixed at 100.

[23] In Figure 10, it is immediately clear that trajectories of particle 3 and particle 4 represent the mainstream of Kuroshio. However, it is worth specially noting that the trajectory of particle 1 passes over the trajectory of particle 2 and extends along the isobath of ∼100 m, while particle 2 intrudes northwestward gradually across the isobaths of 200 and 100 m, and finally reaches the isobath of 50 m, although the initial position of particle 2 is ∼170 m deeper than that of particle 1. The trajectories of particle 1 and particle 2 are significantly different to the current pattern such as KBC and KBCNT (see Figure 1) [*Ichikawa and Beardsley*, 2002; *Qiu and Imasato*, 1990]. Furthermore, the salinity at the initial position of particle 1 is ∼34.6 (see Figure 3f), which is surprisingly consistent to observed maximum salinity of 34.6 at the bottom layer of station DH37. According to the initial depths and the trajectories of particle 1 and particle 2 (see Figure 10), it is immediately clear that the bottom water between station DH32 and DH33 will be colder and less saline than that at the bottom layer of DH37. As the $[PO4]^{3-}$ concentration increases with the water depth in the Kuroshio water (Figure 3g), on the basis of the trajectories of particle 1 and particle 2, it can be reasonably expected that the $[PO4]^{3-}$ concentration between station DH32 and DH33 will be higher than that at the bottom layer of DH37. For these reasons, it is most reasonable that in the bottom water of southern ECS, Kuroshio does exhibit its intrusion by OKBC and NKBC in summer. In addition, the paths of OKBC and NKBC are believed to be represented by the trajectories of particle 1 and particle 2, respectively.

[24] Figures 11a and 11b show the modeled 5 day (20–25 August 2009) average tracer value distributions at bottom layer and along the transect DH3, respectively. In Figure 11a, there are two high–tracer value strips on the southern ECS continental shelf, which properly agree with the high salinity water distribution in Figure 4a. One strip extends continuously into transect DH3 along the 100 m isobath and provides the bottom water of station DH33 with high trace value. At the same time, the other one upwells gradually from ∼250 to ∼60 m, and passes through the transect DH3 between station DH32 and DH33 forming the high tracer water there. It is worth noting that in Figure 11a,

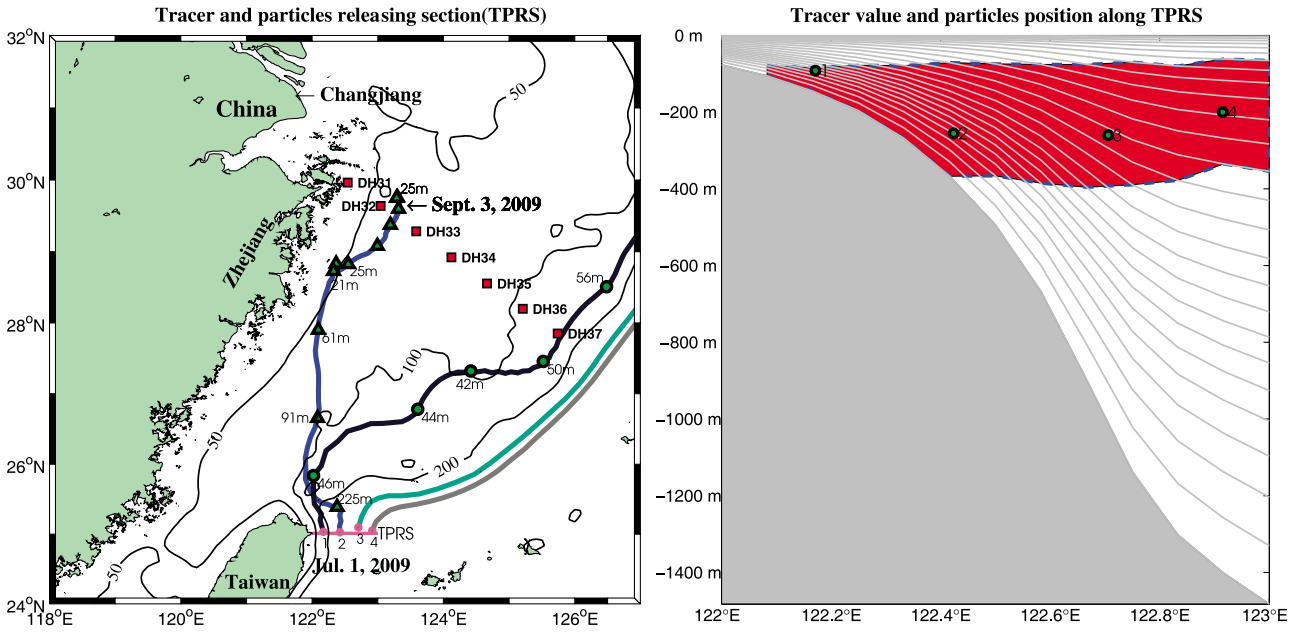

Figure 10. (left) Lagrange trajectories of particles where circles and triangles, together with the depth of particles, are marked every 6 days. Numbers (1, 2, 3, and 4) indicate the initial location of particles, and thin lines denote the isobaths of 50 m, 100 m, and 200 m. (right) The red filled area denotes the area where the tracer with value 100 is released continuously from 1 July to 1 October 2009, and thin lines are terrain following sigma coordinates.

the distribution of the high tracer value along the isobath of 100 m is clearly different when compared with the mainstream of Kuroshio and seems to turn anticlockwise on passing through transect DH3. When Figure 11b is compared with Figure 3b, there is a perfect agreement between the pattern of high-salinity water and the distribution of high–tracer value water. In addition, the central part of Figure 11b is occupied by low–tracer value water, which corresponds to the low-salinity and high-temperature TWCW in Figures 3a and 3b. Either the horizontal features or the vertical characteristics of observations are well reproduced by the tracer experiment. Again, tracer experiments provide evidence for the paths and origins of OKBC and NKBC. In addition, the internal tides have important effect on the pattern of cold domes, but it is not the dominant control factor for the existence of OKBC and NKBC (figures not shown).

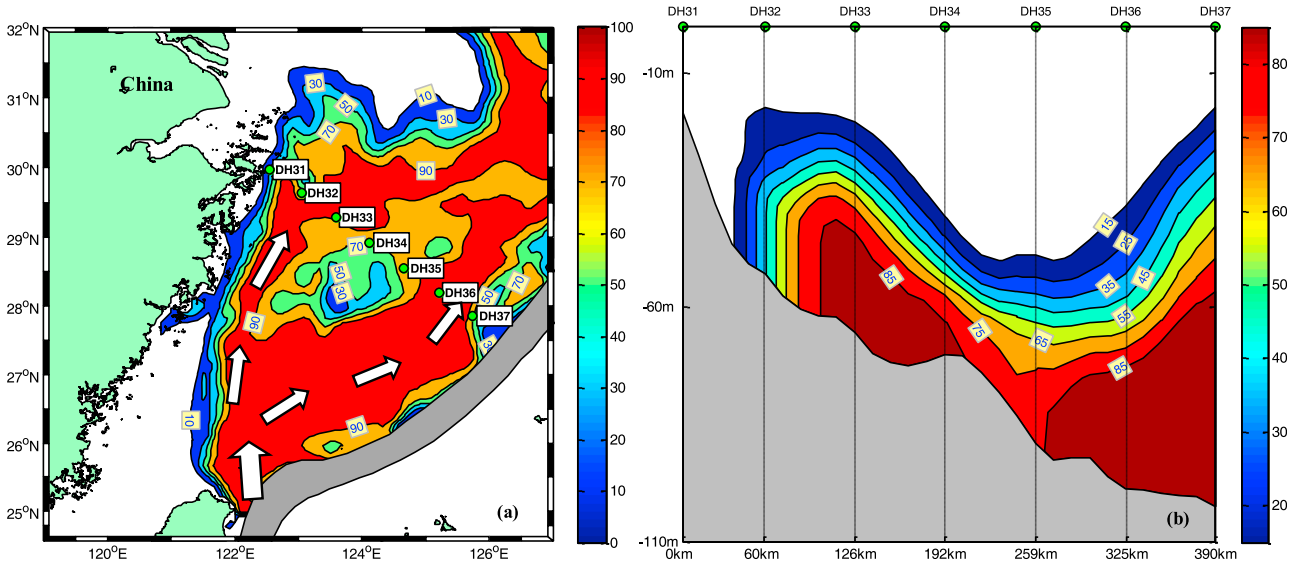

Figure 11. Modeled 5 day (20–25 August 2009) average tracer value distributions at (a) bottom layer along with the station locations of DH3, and (b) along the transect DH3. Gray band in Figure 11a indicates the typical Kuroshio path.

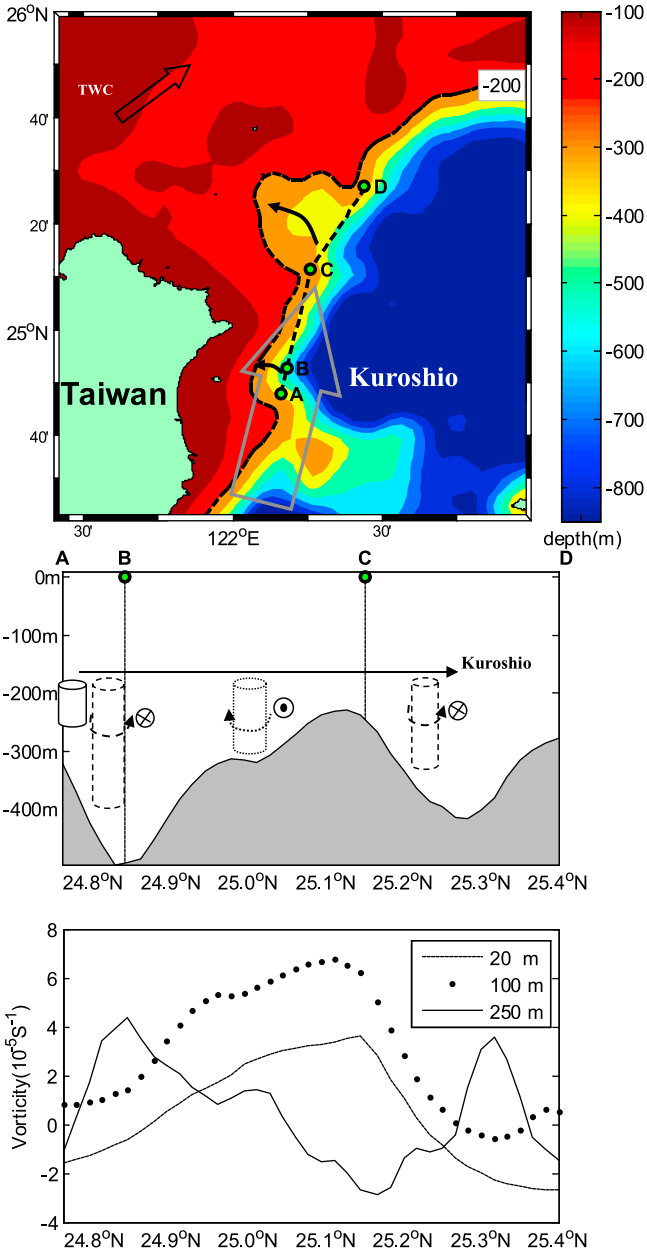

Figure 12. (top) Topography east of Taiwan where isobaths of 200 m is shown and depth deeper than 1000 m is set to 1000 m for simplification. (middle) The topography along the line A-B-C-D and the generation mechanism of Kuroshio branches northeast of Taiwan. (bottom) Dashed, dotted and solid lines show the vorticity along the A-B-C-D line at 20 m, 100 m and 250 m, respectively.

[25] So far, all the observed phenomena in transect DH3 can be well explained on the basis of our assumption that in the bottom water of southern ECS, the Kuroshio mainly exhibits its intrusion by OKBC and NKBC in summer, the origin depth of OKBC is deeper than that of NKBC, and the NKBC and OKBC intrude onto the ECS continental shelf following the trajectories of particle 1 and particle 2, respectively.

4.2. Generation of NKBC and OKBC

[26] To the south of I-Lan Ridge (see Figure 12), the Kuroshio mainly flows along the coast of Taiwan [*Hu et al.*, 2008; *Tang et al.*, 2000], but it departs from the Taiwan coast when it passes over the I-Lan Ridge (see Figure 12, top), and turns to east at ~25.7°N because of zonal-running shelf break there (see Figure 12, top). As a strong thermocline is developed in summer, the movement of upper ocean water above the thermocline is independent of the interaction between Kuroshio and topography [*Chern and Wang*, 1994]. When the mainstream of Kuroshio passes over the I-Lan Ridge, in the Kuroshio water below the thermocline, there is a positive *vortex-tube stretching* [*Pedlosky*, 1979] as a result of the steep slope on the northern side of the I-Lan Ridge, where the depth sharply changes from only ~300 m at I-Lan Ridge to ~500 m (see Figure 12, middle). Then, cyclonical vorticity will be naturally produced between point A and point B (see Figure 12). Therefore, the water near point B will have a tendency to intrude westward, but it is in turn deflected at the shelf break, forming a cyclonic current to the west of Kuroshio [*Chuang et al.*, 1993; *Hsueh et al.*, 1992, 1993; *Liu et al.*, 2000; *Tang and Yang*, 1993; *Tang et al.*, 1999]. Next, as the Kuroshio subsurface water approaches point C, the westward intrusion will turn anticyclonicly and flow northwestward according to the negative *vortex-tube stretching* [*Pedlosky*, 1979] between point B and point C. At the same time, it is interesting to note that there is a canyon between point C and point D (see Figure 12). Thus, the Kuroshio subsurface water will subject to a cyclonic vorticity, when it flows down the slope between point C and point D. Therefore, the westward intrusion of Kuroshio is further reinforced by the slope between point C and point D, which yields a positive vorticity by the downward slope and a negative vorticity by the upward slope (see Figure 12, middle). The above inference is immediately confirmed by the modeled monthly mean vorticity in August 2009 along the A-B-C-D line (see Figure 12, bottom). Along the line A-B-C-D, the modeled vorticity distribution at 250 m depth is out of phase with the variation of the topography. In other words, when there is a trough in the topography, there is a peak in the vorticity distribution. In contrast, the modeled vorticity distributions at 20 and 100 m depths are almost in phase with the elevation of the topography. The intrusion dynamics of deep water (below the thermocline) is obviously different from that of surface water (above the thermocline).The vorticity distribution in the deep water agrees closely with the analysis of the *vortex-tube stretching*. Therefore, it is very reasonable that around point C, there is a strong on-shelf intrusion of Kuroshio subsurface water through the canyon between point C and point D (see Figure 12). The domain between point B and point C may be the place where the NKBC originates. In addition, the topography Rossby wave caused by the variation of *ambient potential vorticity* [*Pedlosky*, 1979; *Isobe*, 2004] maybe plays an important role on the intrusion path of NKBC.

[27] However, when the mainstream of Kuroshio passes over the I-Lan Ridge, the Kuroshio water between 120 and 60 m will continuously intrude northward as a result of its inertia. In addition, when the Kuroshio water (60–120 m) has passed by the coast of the Taiwan, it immediately loses the blocking of the coast of Taiwan. Part of it will turn

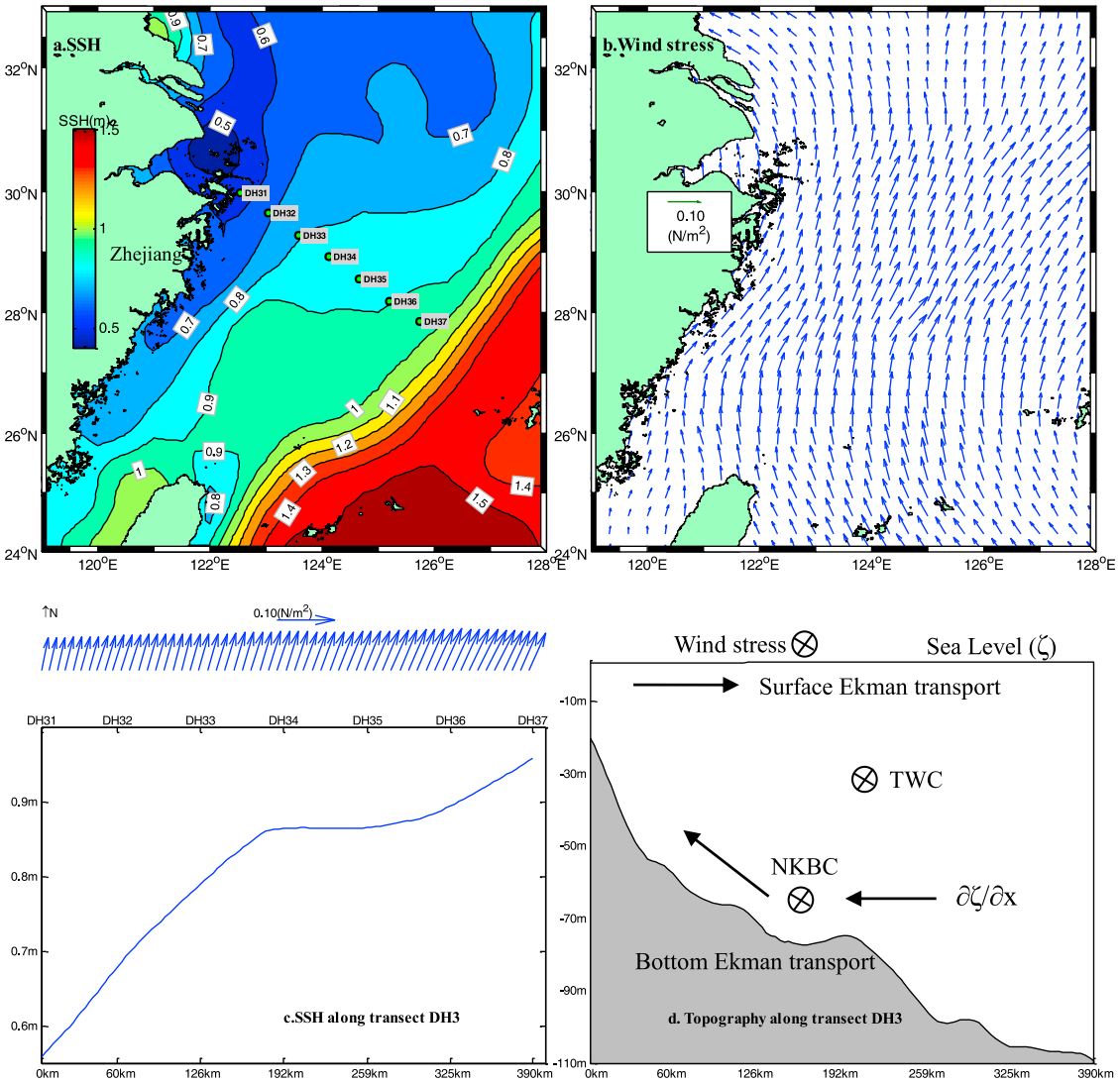

Figure 13. (a) Monthly mean Sea Surface Height (SSH) in August 2009 from AVISO along with the station locations of DH3; (b) monthly mean wind stress in August 2009 from CERSAT; (c) wind stress and SSH along transect DH3; and (d) a diagram explaining why the NKBC can be sustained.

cyclonically because of the westward pressure, which is unbalanced because of the absence of the blocking of the coast of Taiwan. The westward pressure is caused by the higher SSH at the eastern side of Kuroshio than that at the western side (Figure 13a). The OKBC is generated from the cyclonic turning of this part of Kuroshio water (60–120 m). Then, to conserve its potential vorticity, the OKBC turns anticyclonicly and flows following the isobath of 100 m. In contrast, the Kuroshio water above ~60 m, blocked by the TWC and constrained by *β-effect* and the Taiwan island [*Qiu and Imasato*, 1990], turns to east immediately northeast of Taiwan, forming the KBC (see Figure 1).

4.3. Sustaining of NKBC

[28] Figure 13a shows the monthly mean SSH in August 2009, which comes from Archiving, Validation, and Interpretation of Satellite Oceanographic (AVISO) data (http://www.aviso.oceanobs.com/en/data/). It is clear that there is an obvious SSH difference between station DH31 and the area east of Taiwan. According to the southwest monsoon in summer (see the wind stress in Figure 13b, which is from the Centre ERS d'Archivage et de Traitement (CERSAT), http://www.ifremer.fr/cersat/en/data/data.htm), there will be a seaward Ekman transport in the upper ocean water of ECS, and the surface Ekman transport in turn causes the sea level to increase at the eastern side of transect DH3 and decrease at the western side of transect DH3 (see Figure 13c). To conserve mass, off the coast of Zhejiang the bottom water will upwell into the surface Ekman layer at a rate proportional to the divergence of the Ekman flux. Therefore, the intrusion of NKBC will benefit from the pressure gradient and the surface Ekman transport to break the constraint of potential vorticity.

[29] However, when NKBC flows through the transect DH3, there will be a shoreward bottom Ekman transport. It is reasonable that the high-density water in core1 of transect DH3 (see Figure 3a) has a tendency to flow down the west–east running slop (see Figure 13d) to deep water. However,

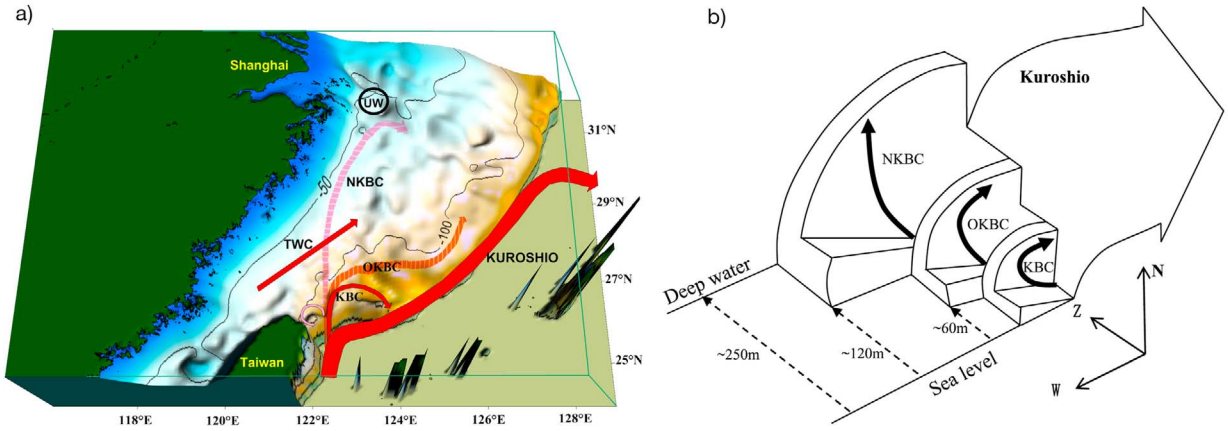

Figure 14. (a) The summer Kuroshio branch pattern where depth more than 500 m is equal to 500 m for simplification, and UW denotes upwelling. Solid thin lines represent the isobaths of 50 m, 100 m, and 200 m. (b) The vertical structure of the Kuroshio branches where N, W, and Z denote north, west, and depth directions, respectively.

the current pattern of NKBC is sustained because the downslop tendency is balanced by the shoreward pressure gradient together with the surface and bottom Ekman transport.

5. Conclusion

[30] On the basis of field observations and numerical simulation, we propose that, in summer, the pattern of Kuroshio intrusion branches on the southern ECS continental shelf can be mostly represented by four branches: KBC [*Qiu and Imasato*, 1990], OKBC, NKBC, and the westward Kuroshio branch [*Chuang et al.*, 1993; *Hsueh et al.*, 1993] to the west of KBC (see Figure 14a). The OKBC flows nearly along the isobath of ~100 m, while the NKBC upwells northwestward gradually from northeast of Taiwan to the coast of Zhejiang province, China, and finally turns to the east off Changjiang river mouth at 30.5°N (see Figure 14a). It is worth noting that either the OKBC or the NKBC is clearly different compared with previous studies such as KBC [*Qiu and Imasato*, 1990] and KBCNT [*Ichikawa and Beardsley*, 2002; *Kondo*, 1985].

[31] The OKBC stems mostly from the Kuroshio water between ~60 and ~120 m, which is generated by the combined effects of topography, *β-effect*, and the blocking of TWC. Moreover, the NKBC originates mainly in the Kuroshio subsurface water between ~120 and ~250 m, which is mostly caused by the interaction between the Kuroshio and the topography.

[32] The vertical structure of the Kuroshio intrusion branches are shown in Figure 14b, where the Kuroshio exhibits its intrusion branches on southern ECS continental shelf by an anticyclonical stair structure: bottom stair NKBC, middle stair OKBC, and top stair Kuroshio surface branch (KBC). Furthermore, the observed colder, less saline, and more phosphate-rich water in core1 rather than in core2 can be explained very well by this pattern of OKBC and NKBC.

[33] In addition, in summer, the cross-shelf NKBC and OKBC are obviously the main pathways through which the materials (such as phosphate) in the deep water of west Pacific Ocean can be transported continuously into the ECS across the Kuroshio. In turn, the material will play an important role in the biological system of ECS.

[34] **Acknowledgments.** This paper was supported by National Natural Science Foundation of China through grant 40806009, 973 Project (2009CB421205), National Natural Science Foundation of China through grant 40976008, Innovation Project of Chinese Academy of Sciences (KZCX2-EW-209), Innovation Group Project of Chinese Academy of Sciences (KZCX2-YW-Q07-01), and National Basic Research Program of China (project 2012CB956000). This paper was supported by High Performance Computing Center, Institute of Oceanology, Chinese Academy of Sciences. We acknowledge Minhan Dai from Xiamen University for his phosphate data.

References

Chang, Y. L., and L. Y. Oey (2011), Interannual and seasonal variations of Kuroshio transport east of Taiwan inferred from 29 years of tide-gauge data, *Geophys. Res. Lett.*, *38*, L08603, doi:10.1029/2011GL047062.

Chen, C. T. A., R. Ruo, S. C. Pai, C. T. Liu, and G. T. F. Wong (1995), Exchange of water masses between the East China Sea and the Kuroshio off northeastern Taiwan, *Cont. Shelf Res.*, *15*(1), 19–39, doi:10.1016/0278-4343(93)E0001-O.

Chern, C.-S., and J. Wang (1994), Influence of the seasonal thermocline on the intrusion of Kuroshio across the continental shelf northeast of Taiwan, *J. Oceanogr.*, *50*(6), 691–711, doi:10.1007/BF02270500.

Chuang, W. S., H. W. Li, T. Y. Tang, and C. K. Wu (1993), Observations of the countercurrent on the inshore side of the Kuroshio northeast of Taiwan, *J. Oceanogr.*, *49*, 581–592, doi:10.1007/BF02237464.

Egbert, G. D., and S. Y. Erofeeva (2002), Efficient inverse modeling of barotropic ocean tides, *J. Atmos. Oceanic Technol.*, *19*(2), 183–204, doi:10.1175/1520-0426(2002)019<0183:EIMOBO>2.0.CO;2.

Grasshoff, K., M. Ehrhardt, and K. Kremling (1983), *Methods of Seawater Analysis*, Verlag Chemie, Weinheim, Germany.

Guan, B. X., and G. H. Fang (2006), Winter counter-wind currents off the southeastern China coast: A review, *J. Oceanogr.*, *62*(1), 1–24, doi:10.1007/s10872-006-0028-8.

Guo, X. Y., H. Hukuda, Y. Miyazawa, and T. Yamagata (2003), A triply nested ocean model for simulating the Kuroshio: Roles of horizontal resolution on JEBAR, *J. Phys. Oceanogr.*, *33*(1), 146–169, doi:10.1175/1520-0485(2003)033<0146:ATNOMF>2.0.CO;2.

Guo, X. Y., Y. Miyazawa, and T. Yamagata (2006), The Kuroshio onshore intrusion along the shelf break of the East China Sea: The origin of the Tsushima Warm Current, *J. Phys. Oceanogr.*, *36*(12), 2205–2231, doi:10.1175/JPO2976.1.

Hasumi, H., H. Tatebe, T. Kawasaki, M. Kurogi, and T. T. Sakamoto (2010), Progress of North Pacific modeling over the past decade, *Deep Sea Res., Part II*, *57*(13–14), 1188–1200, doi:10.1016/j.dsr2.2009.12.008.

Hsueh, Y., C. S. Chern, and J. Wang (1993), Blocking of the Kuroshio by the continental-shelf northeast of Taiwan, *J. Geophys. Res.*, *98*(C7), 12,351–12,359, doi:10.1029/93JC01075.

Hsueh, Y., J. Wang, and C. S. Chern (1992), The intrusion of the Kuroshio across the continental-shelf northeast of Taiwan, *J. Geophys. Res.*, *97*(C9), 14,323–14,330, doi:10.1029/92JC01401.

Hu, D. X., L. H. Lu, Q. C. Xiong, Z. X. Ding, and S. C. Sun (1984), On the cause and dynamical structure of the coastal upwelling off Zhejiang province (in Chinese), *Stud. Mar. Sin.*, *21*, 101–112.

Hu, J. Y., H. Kawamura, C. Y. Li, H. S. Hong, and Y. W. Jiang (2010), Review on current and seawater volume transport through the Taiwan Strait, *J. Oceanogr.*, *66*(5), 591–610, doi:10.1007/s10872-010-0049-1.

Hu, X. M., X. J. Xiong, F. L. Qiao, B. H. Guo, and X. P. Lin (2008), Surface current field and seasonal variability in the Kuroshio and adjacent regions derived from satellite-tracked drifter data, *Acta Oceanol. Sin.*, *27*(3), 11–29.

Ichikawa, H., and R. Beardsley (2002), The current system in the Yellow and East China Seas, *J. Oceanogr.*, *58*(1), 77–92, doi:10.1023/A:1015876701363.

Isobe, A. (2004), Driving mechanism of band structure of mean current over the continental shelf, *J. Phys. Oceanogr.*, *34*(8), 1839–1855.

Isobe, A. (2008), Recent advances in ocean-circulation research on the Yellow Sea and East China Sea shelves, *J. Oceanogr.*, *64*(4), 569–584, doi:10.1007/s10872-008-0048-7.

Johns, W. E., T. N. Lee, D. X. Zhang, R. Zantopp, C. T. Liu, and Y. Yang (2001), The Kuroshio east of Taiwan: Moored transport observations from the WOCE PCM-1 array, *J. Phys. Oceanogr.*, *31*(4), 1031–1053, doi:10.1175/1520-0485(2001)031<1031:TKEOTM>2.0.CO;2.

Kondo, M. (1985), Oceanographic investigation of fishing grounds in the East China Sea and Yellow Sea—Part I. Characteristics of the mean temperature and salinity distributions measured at 50 m and near the bottom [in Japanese with English abstract], *Bull. Sekai Reg. Fish. Lab.*, *62*, 19–55.

Large, W. G., J. C. McWilliams, and S. C. Doney (1994), Oceanic vertical mixing: A review and a model with a nonlocal boundary layer parameterization, *Rev. Geophys.*, *32*(4), 363–403, doi:10.1029/94RG01872.

Liang, W. D., T. Y. Tang, Y. J. Yang, M. T. Ko, and W. S. Chuang (2003), Upper-ocean currents around Taiwan, *Deep Sea Res., Part II*, *50*(6–7), 1085–1105, doi:10.1016/S0967-0645(03)00011-0.

Liu, K. K., G. C. Gong, S. Lin, C. Y. Yang, C. L. Wei, S. C. Pai, and C. K. Wu (1992), The year-round upwelling at the shelf break near the northern tip of Taiwan as evidenced by chemical hydrography, *Terr. Atmos. Oceanic Sci.*, *3*, 243–276.

Liu, K. K., T. Y. Tang, G. C. Gong, L. Y. Chen, and F. K. Shiah (2000), Cross-shelf and along-shelf nutrient fluxes derived from flow fields and chemical hydrography observed in the southern East China Sea off northern Taiwan, *Cont. Shelf Res.*, *20*(4–5), 493–523, doi:10.1016/S0278-4343(99)00083-7.

Marchesiello, P., J. C. McWilliams, and A. Shchepetkin (2001), Open boundary conditions for long-term integration of regional oceanic models, *Ocean Modell.*, *3*(1–2), 1–20, doi:10.1016/S1463-5003(00)00013-5.

Pedlosky, J. (1979), *Geophysical Fluid Dynamics*, Springer, New York.

Qiu, B., and N. Imasato (1990), A numerical study on the formation of the Kuroshio counter current and the Kuroshio branch current in the East China Sea, *Cont. Shelf Res.*, *10*(2), 165–184, doi:10.1016/0278-4343(90)90028-K.

Shchepetkin, A. F., and J. C. McWilliams (2005), The regional oceanic modeling system (ROMS): A split-explicit, free-surface, topography-following-coordinate oceanic model, *Ocean Modell.*, *9*(4), 347–404, doi:10.1016/j.ocemod.2004.08.002.

Shchepetkin, A. F., and J. C. McWilliams (2009), Correction and commentary for "Ocean forecasting in terrain-following coordinates: Formulation and skill assessment of the regional ocean modeling system," *J. Comput. Phys.*, *228*(24), 8985–9000, doi:10.1016/j.jcp.2009.09.002.

Song, Y. H., and D. Haidvogel (1994), A semiimplicit ocean circulation model using a generalized topography-following coordinate system, *J. Comput. Phys.*, *115*(1), 228–244, doi:10.1006/jcph.1994.1189.

Su, J. L., Y. Q. Pan, and X. S. Liang (1994), Kuroshio intrusion and Taiwan Warm Current, in *Oceanology of China Seas*, vol. 1, edited by D. Zhou et al., pp. 59–77, Kluwer Acad., Dordrecht, Netherlands.

Su, Y. S., and X. C. Wong (1994), Water masses in China Seas, in *Oceanology of China Seas*, vol. 1, edited by D. Zhou et al., pp. 3–6, Kluwer Acad., Dordrecht, Netherlands.

Takikawa, T., J. H. Yoon, and K. D. Cho (2005), The Tsushima warm current through Tsushima Straits estimated from ferryboat ADCP data, *J. Phys. Oceanogr.*, *35*(6), 1154–1168, doi:10.1175/JPO2742.1.

Tang, T. Y., and Y. J. Yang (1993), Low frequency current variability on the shelf break northeast of Taiwan, *J. Oceanogr.*, *49*, 193–210, doi:10.1007/BF02237288.

Tang, T. Y., Y. Hsueh, Y. J. Yang, and J. C. Ma (1999), Continental slope flow northeast of Taiwan, *J. Phys. Oceanogr.*, *29*(6), 1353–1362, doi:10.1175/1520-0485(1999)029<1353:CSFNOT>2.0.CO;2.

Tang, T. Y., J. H. Tai, and Y. J. Yang (2000), The flow pattern north of Taiwan and the migration of the Kuroshio, *Cont. Shelf Res.*, *20*(4–5), 349–371, doi:10.1016/S0278-4343(99)00076-X.

Teague, W. J., G. A. Jacobs, D. S. Ko, T. Y. Tang, K. I. Chang, and M. S. Suk (2003), Connectivity of the Taiwan, Cheju, and Korea straits, *Cont. Shelf Res.*, *23*(1), 63–77, doi:10.1016/S0278-4343(02)00150-4.

Wong, G. T. F., S. Y. Chao, Y. H. Li, and F. K. Shiah (2000), The Kuroshio edge exchange processes (KEEP) study: An introduction to hypotheses and highlights, *Cont. Shelf Res.*, *20*(4–5), 335–347, doi:10.1016/S0278-4343(99)00075-8.

Yang, D., B. Yin, Z. Liu, and X. Feng (2011), Numerical study of the ocean circulation on the East China Sea shelf and a Kuroshio bottom branch northeast of Taiwan in summer, *J. Geophys. Res.*, *116*, C05015, doi:10.1029/2010JC006777.

Zhang, D. X., T. N. Lee, W. E. Johns, C. T. Liu, and R. Zantopp (2001), The Kuroshio east of Taiwan: Modes of variability and relationship to interior ocean mesoscale eddies, *J. Phys. Oceanogr.*, *31*(4), 1054–1074, doi:10.1175/1520-0485(2001)031<1054:TKEOTM>2.0.CO;2.

T. Bai, North China Sea Marine Forecasting Center, State Oceanic Administration, Qingdao 266033, China. (baitao@nmfc.gov.cn)

H. Chen, Z. Liu, J. Qi, D. Yang, and B. Yin, Institute of Oceanology, Chinese Academy of Sciences, 7 Nanhai Rd., Qingdao 266071, China. (hychen@qdio.ac.cn; zhlliu@qdio.ac.cn; qijifeng80@163.com; yangdezhou@qdio.ac.cn; bsyin@qdio.ac.cn)